23 Brain Diseases

MOHAMED A. SHERIF AND WILLIAM W. LYTTON

One major approach to computational neuroscience utilizes multiscale modeling, covering molecular, cellular, and network phenomena as well as higher levels up to cognition and behavior. With growing appreciation of the enormous complexity of genome, proteome, and other -omes, multiscale modeling is becoming increasingly important in clinical medicine. These complexities are even more apparent when confronting brain diseases, dysfunctions of the most complex organ, an organ with manifestations that range up into the realms of cognition and behavior.

Different tools, used to explore different aspects of the brain, obtain data at different scales. Some of these are used only in experimental animals, such as visualization of intracellular calcium activation waves. Others can be used both experimentally and clinically in humans, such as electrophysiological recordings and functional or structural neuroimaging.

Additionally, different disease phenomena cover a range of temporal and spatial scales. This is true for both pathogenesis and pathophysiology (describing the mechanisms of how disease occurs) and treatment, whether it is pharmacological, behavioral, or surgical. Disease can start at a molecular or cellular level and then produce effects all the way up across different temporal and spatial scales, till reaching the systems level of the whole organism. Alternatively, disease may start at a high level (e.g., traumatic brain injury and stroke) and produce alterations at cellular and molecular levels. Similarly, bottom-up and top-down approaches to treatment may be used simultaneously. For example, drug therapy for psychiatric diseases is applied to molecular targets in concert with behavioral or cognitive therapy that is aimed at altering the function of brain maps and brain circuitry.

We will discuss four brain disorders. We start with epilepsy, arguably the most dynamically simple of brain diseases. We will discuss how computational neuroscience has aided in exploring the predictability of occurrence of seizures, and how it helped in investigating factors related to network excitability that may predispose someone to seizures. We then move to Parkinson's disease (PD), a neurodegenerative disease manifested by tremor and slowness of movement. Computational modeling of the basal ganglia circuits in the brain has helped to point out why many PD patients suffer from problems with learning new tasks, even after being treated. The next disease we explore is stroke, looking at models of the changes that occur following these major brain ablations. We look at how the death of neurons shifts the dynamics of cortical neurons, which helps reduce loss of function. Additionally, models of the effect of physiotherapy on patients with stroke made interesting predictions with implications for patterning physical therapy after stroke. Finally we discuss computational modeling of schizophrenia. Further understanding of this devastating illness may help us shed light on the enigma of thought disorders and through this, better understand the processes of normal cognition.

For the reasons given above, this chapter will focus on multiscale modeling. However, we will say relatively little about high-level approaches that describe disease in terms of chaotic dynamics (Glass and Mackey, 1988). Although these and other top-down approaches have provided a number of important insights, we have chosen to focus on multiscale modeling because of its potential clinical applicability through new approaches to developing pharmacological treatments.

23.1 Epilepsy

23.1.1 Pathophysiology of Seizures Seizures are episodes of disturbed brain function due to abnormal prolonged neuronal firing. Seizures can cause simple changes in attention and behavior or a complete disruption of brain activity with loss of consciousness and abnormal movements of the limbs. The location of a localized (focal) seizure determines the brain function that is affected. For example, if the seizure location involves the motor cortex, then the disturbance of function will be in the form of involuntary jerking movements of the body part innervated by that area of the cortex. If the seizure location involves the sensory

cortex, then it will present as abnormal sensations in the body region represented in that area. Generalized seizures involve the whole brain and result in loss of consciousness. When seizures occur repeatedly without provocation, the disease is called epilepsy. Usually, the abnormal firing during seizures will stop after a period of time, and so the symptoms will stop, too. However, if the symptoms persisted for a long period of time, it is called status epilepticus.

A common seizure presentation is the generalized tonic–clonic seizure. Tonic refers to sustained muscular contraction while clonic refers to alternating contraction and relaxation of muscles. During a generalized tonic–clonic seizure, the patient suddenly loses consciousness, followed by a generalized contraction of all body musculature for around 10–20 seconds. The patient's body becomes rigid, sometimes with arching of the back and neck (tonic phase). This is followed by alternating contraction and relaxation of body musculature (clonic phase), resulting in rhythmic recurrent movements of the limbs and body, known as convulsions. Convulsion frequency then decreases gradually until the seizure ends over a period of 1 to 2 minutes. If the seizure instead continues over many minutes, this is status epilepticus, and it is a life-threatening condition.

Multiple elements at different scales are involved in the pathophysiology of epilepsy. The occurrence of seizures is related not only to increased excitability of individual neurons but also to altered neuronal dynamics within the network. Multiscale modeling provides a method to meet the challenge of understanding how these many elements interact to produce the disorder, assimilating different areas of neuroscience, ranging from neurogenetics and ion channel dynamics to brain imaging, electroencephalography (EEG), and behavioral assessments. Because the presenting "behavior" (a convulsion) is extremely simple relative to motivated behaviors, the correlation between basic science and clinical phenomenology is closer in epilepsy than in other brain disorders. There has therefore been more success in linking molecular and cellular pathophysiology to clinical symptoms and signs in this disease. Modeling allows us to explore the effect of changes taking place along one or more of these space-time scales on the generation of network spontaneous repetitive activity.

The pathology responsible for the occurrence of seizures is rarely limited to one structure. The pathology can be in any structure ranging from the ionic channels within the neuronal membrane, going all the way up to the connectivity within a neuronal network or the connectivity between networks. For example, a group of diseases known as channelopathies (diseases of the channels) consists of mutations affecting the structure of the ion channels. This results in changes in their conductance, either increasing or decreasing it. The effect of such changes on neuronal excitability depends on the role of the particular channel in membrane depolarization/hyperpolarization. Another example is the effect of chronic alcohol (ethanol) use on $GABA_A$ receptors. Alcohol binds to the $GABA_A$ receptor complex, which is a chloride channel, augmenting its function and increasing the influx of chloride ions, resulting in inhibition of neuronal firing. Chronic alcohol exposure reduces $GABA_A$-receptor-mediated inhibition (Kang et al., 1996). Therefore, abrupt cessation of alcohol intake following chronic alcohol use can result in neuronal hyperexcitability with resultant seizures.

Abnormalities of network architecture have also been reported in epilepsy. Some cases of seizures can't be controlled with medications. In these cases, surgery is done to attempt to remove brain tissue that has been identified as the focus generating the seizure. Examination of the brain tissue removed reveals abnormalities of network architecture in humans. Similar abnormalities are also seen in animal models of epilepsy. These changes include sprouting of new fibers to make atypical connections, as well as the presence of cells in abnormal locations (Sutula et al., 1989; Parent et al., 1997).

23.1.2 Stochastic and Deterministic Modeling

Both stochastic and deterministic modeling have their role in investigating questions related to seizures and epilepsy. Underlying randomness may be real, as in the case of random opening and closing of individual ion channels. However, stochastic modeling is also often used when a system is too complex to consider modeling the underlying details, or when a system is subject to vagaries that cannot reasonably be modeled. This randomness is only apparent, due to incomplete information or due to sensitivity to initial conditions as in chaotic systems. Stochastic models are therefore helpful even in deterministic systems, capturing irreducible complexity that may determine specific aspects of epilepsy, such as the timing of seizures. For example, seizures are known to be more likely to occur after a night's sleep has been missed. Since we do not know exactly how this missed night's sleep is affecting the brain, it is not feasible to model all the details that could be affected. Such phenomena could be modeled using stochastic models.

The enormous dynamical complexity of the brain, like its structural complexity, can be considered as a set

of subsystems. The existence of widespread distinct oscillatory frequencies in the EEG (see chapter 4, "Neural Rhythms") suggests that dynamical subsystems are detectable even at the highest scale. Hence, it has been proposed that the enormous dimensionality of the brain produces trajectories that lie in much lower-dimensional subspaces that can then be modeled by equivalent low-dimensional dynamical systems. Following this hypothesis, low-dimensional mean-field models (also called neuron population models or lumped models) have been widely utilized to simulate seizures.

These models look at the overall dynamics of a large ensemble of neurons—the lump. Depending on the model, this neural lump could be interpreted to be a cortical minicolumn, a column, a Brodmann area, a thalamic nucleus, and so forth. Alternatively, a lump could be a pool of similar neurons, typically an inhibitory pool coupled with an excitatory pool. These models have an advantage of simplicity compared to detailed neural-level modeling, making it is easier to simulate multiple brain regions.

Seizure spread is a clinically significant phenomenon, affected by multiple factors. Seizures can spread in a series of stages: a focal seizure with secondary generalization. For example, in temporal lobe epilepsy, a patient may experience "auras," unusual feelings such as déjà vu (a sense of familiarity to an unfamiliar situation), jamais vu (the opposite of déjà vu, a sense of unfamiliarity to familiar situations), or fear, at the beginning of abnormal neural firing in the temporal lobe. These are then followed by loss of consciousness as the wave of abnormal neuronal firing spreads broadly into the neocortex. Alternatively, a seizure can appear to arise suddenly in all areas, a primary generalized seizure. For example, in absence epilepsy, a classical generalized epilepsy usually seen in children, the child suddenly stops whatever he or she is doing, stares ahead, and becomes unresponsive for about a minute. Although seizure spread in generalized epilepsy occurs so quickly as to appear to be simultaneous across brain areas, there is evidence that generalized epilepsy instead involves very rapid spread.

23.1.3 Modeling Neuronal Populations To investigate some of the mechanisms playing a role in the spread of a seizure, Larter et al. modeled the CA3 region of the hippocampus (Larter et al., 1999). The model consisted of connected modules, with each module consisting of a lumped excitatory population and a lumped inhibitory population. The excitatory population activation was described by differential equations which depended on calcium, potassium, and leak currents:

$$\frac{dV_i}{dt} = -g_{Ca} m_\infty (V_i - 1) - g_K W_i (V_i - V_i^K) - g_L (V_i - V^L) + 1 - \alpha_{inh} Z_i \tag{23.1}$$

where V is the voltage of the lumped pyramidal cell population and g_{Ca}, g_K, and g_L are the total conductances for calcium, potassium, and leak channels, respectively. W_i is the fraction of open potassium channels in the lumped pyramidal neurons. m_∞ is the fraction of open calcium channels and is voltage dependent. V_i^K is the Nernst equilibrium for potassium at node i while V^L is for leak potential. α_{inh} is the inhibitory synaptic strength on the lumped pyramidal neurons, while Z_i is the voltage of lumped inhibitory population at module i. The lumped inhibitory population was modeled similarly.

Activity spread in the model took place at different timescales based on different mechanisms. On a fast timescale, the activity of a module projected to other modules. At a slower timescale, activity results in increased extracellular potassium level, which then diffused to nearby neuronal groups. High extracellular potassium depolarizes the neurons, bringing them closer to threshold for firing, hence more excitable. The Nernst equation describes how different ion concentrations across the cell membrane creates the "batteries" that drive membrane electricity. Depolarization of the membrane with high potassium is then due to a shift of the potassium Nernst potential. To take that into account, V_i^K, in the second term of equation 23.1, was calculated to depend on the activity in the neighboring locations $\overline{V_j}$:

$$V_i^K = \left(\sum_{j=1}^{6} \frac{\overline{V_j}}{6} \right) - \frac{1}{2} \tag{23.2}$$

where

$$\overline{V_j} = \frac{1}{T} \int_{t_{\text{int}}/6}^{t_{\text{int}}} V_j(t) dt \tag{23.3}$$

The t_{int} parameter would determine the duration before the activity is transmitted from one group to another. A short t_{int} allowed the immediate synaptic effect to be more influential. A long t_{int} emphasized the effect of diffusion.

Exploring the range of values of t_{int} revealed two points of bifurcation (see chapter 3, "Neurons and Neuronal Networks as Dynamical Systems"). Below a certain value, all of the modules in the network would fire together, producing a seizure. Above that value, the

network entered a periodic mode, with the modules firing out of phase. This mode was spatially dependent, such that closer modules fired at closer phase than those farther away. At the second point of bifurcation, the network entered a mode of random firing. The authors also explored the effects of inhibition on the firing synchronicity by a variable which governed the ratio of current going into excitatory and inhibitory modules. Lowering the input to inhibitory interneurons relative to excitatory interneurons produced less variability and so made the network more vulnerable to seizure-like activity.

Another factor which influences the spread of seizures is network connectivity. A graph theoretic approach can be used to describe how neurons in a network (or modules in a network of populations) are connected. In graph theory, random networks and small-world networks are the most heavily studied. In a random network, each node has the same probability of being connected to any other node. The notion of a small-world network comes from social networking and other applications where there are special nodes, called hubs, which have more connections to other nodes. In the case of social networks, these hubs are people with lots of friends. In the case of the airport system, these hubs are locations with flights to many other locations. In either case, the hubs provide short paths that connect any two nodes (two people or two airports) in the system.

Another arrangement is hierarchical connectivity. In this arrangement there are clusters of hubs: a cluster is a group of hubs which are heavily interconnected.

In the cerebral cortex, neurons self-organize via synaptic plasticity, producing network organizations that are far from random. However, they can be generally described by graph theory. Cortex is suborganized into subnetworks or modules, with more connections within the module (intramodular) than between the modules (intermodular), suggestive of hierarchical connectivity. The connections at various levels are described in terms of *connectomes* at various levels, within the column, between columns (within area), between areas (within system), and between systems (Sporns et al., 2005; Yoshimura et al., 2005).

Kaiser et al. (2007) compared seizure spread in three types of connectivity: random, small world, and hierarchical. The three types of networks were all of the same size: 1,000 vertices (nodes) and 12,000 edges (connections). Spread of activity was measured as the time to full activation of the whole network.

Spread across the random network topography was the most rapid. Network activity persisted for a longer duration in small-world and hierarchical networks. Compared to small-world networks, networks with hierarchical topography showed more limited activity spread with longer duration. In the case of hierarchical networks, the connections between clusters provided checkpoints of activation before activity could spread across the rest of the network. This suggested that the pace of activity spread in cortex might be limited by the delay in activation of individual columns or local areas before activity can spread further. In this model, there were no inhibitory connections, which shows that the topography of network can limit the spread of seizures even in the absence of inhibitory connections. The visual system has long been considered to be hierarchical, but the macaque data on which this interpretation has been based has been called into question lately by studies that identify a denser pattern of connectivity. Meanwhile human imaging data has suggested to some groups that there may be considerable small-world connectivity among some areas of the brain. Therefore, there remains considerable controversy as to the dominant pattern of connectivity of the connectome.

While the prior study emphasized seizure spread in cortex, other studies have looked at the dynamics of connections between cortex and subcortical structures such as basal ganglia and thalamus. Suffczynski et al. (2004) identified two attractors in a lumped study of interacting cortical and thalamic populations. Both the cortical and thalamic modules consisted of interconnected excitatory and inhibitory populations. Projections between cortex and thalamus were excitatory and projected onto both populations in the other area. The behavior of the model was assessed by evaluating mean activation of the pyramidal (excitatory) cell population of the cortical module.

The resulting system dynamics could maintain physiological activity corresponding to a low-amplitude attractor. Alternatively, a pathological pattern of ictal (seizure-like) activity was produced when dynamics switched over to a high-amplitude attractor. The physiological pattern demonstrated spindle-like oscillations of ~11 Hz frequency, which waxed and waned in amplitude. The pathological pattern showed high-amplitude oscillations of frequency ~9 Hz, which resembled seizure activity (figure 23.1). Transition from the normal nonseizure state to ictal activity occurred when the barrier between these two attractors was overcome. This occurred as the threshold for inhibitory synaptic activation was reached, augmenting oscillation amplitudes. Gaussian white noise introduced into the system could produce transitions from the physiological to the pathological attractor and back. In the absence of noise, the deterministic system remained in the physiological state.

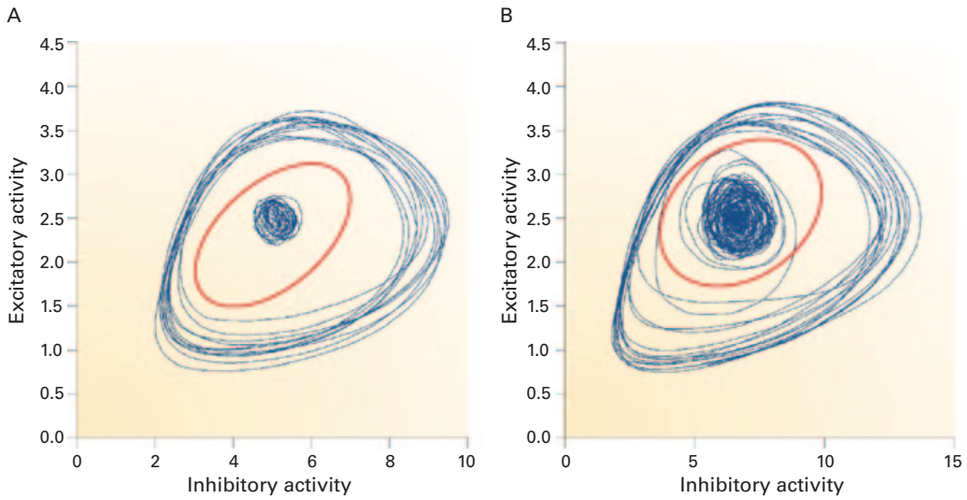

FIGURE 23.1 A lumped model of absence epilepsy. (a) Under deterministic conditions, trajectories (blue line) are stable within their own attractors: the inner attractor represents physiological activity while the outer attractor represents epileptic activity. The red line is the barrier (separatrix) between the attractors. (b) Trajectory jumps repeatedly between attractors as transitions from one attractor to the other are driven by noise. From Lopes Da Silva et al. (2003).

The importance of noise in switching between attractors in this type of model suggests why there might be limitations in the predictability of seizures. Two scenarios suggest themselves. If dynamical changes take place gradually—a physiological attractor evolving gradually into an ictal attractor—then seizures may be predictable. Such a gradual change is hypothesized to occur in temporal lobe epilepsy. By contrast, the dynamics of figure 23.1 shows a *jump* from one attractor to another. Here, the two attractors (ictal and normal) coexist, but are separated from each other by a barrier which is lower in patients suffering from epilepsy, making it easier for the brain state to jump from one attractor to the other. This would explain cases where the onset of seizures can happen very abruptly, as in the case of absence seizures. Additionally, since such jumps happen randomly, it becomes impossible to predict seizures far in advance. Note that in this case, the dynamics of the energy barrier will also play a role and could provide the possibility of prediction of periods of greater susceptibility.

23.1.4 NEURAL-LEVEL MODELING Regardless of the level of detail chosen, all models necessarily contain much simplification. Contrasting with the lumped models described above, more detailed neural-level models incorporate individual neurons but still must simplify in many different ways. For example, molecular interactions are usually not directly simulated. Although these can be helpful to provide direct application to neuropharmacology, simulation using simplified neurons can also be helpful in this respect.

Neural-level models may have both deterministic and stochastic aspects. Local neural activity is represented by differential equations, while stochastic driving is used to represent the variations in external activity patterns from other brain areas. Neural-level models have been used to compare the relative effects of intrinsic neuronal excitability and synaptic connectivity in the genesis of epileptiform activity. In these models, simplification occurs not only from the omission of molecular details but also from simplifications of connectivity due to the fact that there is little that is known about the wiring diagram (the microconnectome) among individual neurons.

As an example, we present here a simplified network consisting of excitatory, inhibitory, and driver neurons which was used to investigate the transition from normal activity to a clonic seizure (Lytton and Omurtag, 2007). The *driver neurons* drove the network through their spontaneous firing. Drivers were connected to both excitatory and inhibitory neurons via different types of excitatory and inhibitory synaptic connections. Individual neurons in this model are event-driven firing units, which fire at a point when the voltage state variable is driven above threshold. Intrinsic properties including the threshold, refractory period, and after-hyperpolarization potential were added to these units through a series of rules.

Two patterns of firing were noted in the network: low-amplitude activity, and prolonged continuous firing, suggestive of tonic epileptiform activity. It was observed that altering the firing timing of the driving neurons, without changing any of the other parameters,

resulted in switching between these two patterns. Another finding of interest was that increasing the excitability of individual neurons did not necessarily result in increasing the excitability of the whole network. This was because the network excitability depended not only on the individual neurons but also on the dynamics between the neurons.

Because neural-level details were used, it was possible to grossly model the effect of anti-epileptic medications. One hypothesized molecular mechanism for anti-epileptic medications is blocking voltage-dependent sodium channels which will reduce the tendency of the neuron to spike (Xie et al., 1995). Using the model, this effect was simulated by simply reducing the excitability of the individual cells by reducing the number of spikes per burst for each unit. This resulted in reduction of the duration of each activation at the neural level but with no effect on the background activity at the population level. Note the similarity of pattern between the two field potentials (blue, untreated; red, treated) in figure 23.2. Note also that the tonic period of pathological activity (arrow) is eliminated in the treated model. Therefore, the tonic seizure was removed by treatment without affecting baseline activity.

When a clinical phenomenon is controlled by a large number of variables, as in the case of epilepsy, computational modeling will aid in our understanding of the interacting and emergent effects of the different state variables at different scales. This would point toward influences that play a bigger role in the phenomenon, enabling research on therapies to focus on these particular state variables at these particular scales.

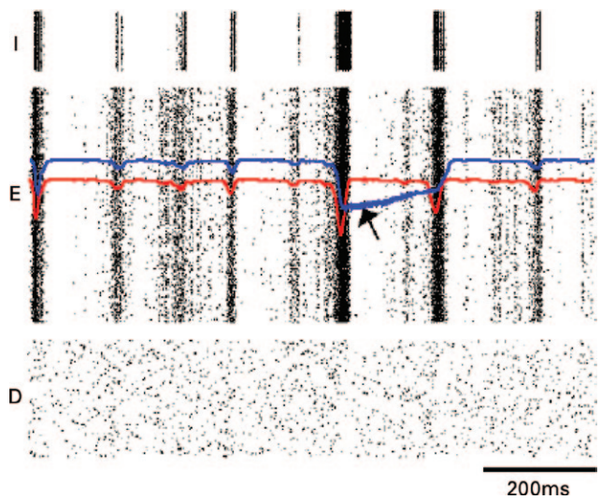

FIGURE 23.2 Effects of anti-epileptic medication. Lines show field potential generated by the activity of a set of expressor neurons (the excitatory neurons) (blue, without medication; red, with medication). Raster plot for the firing of different neuronal subpopulations (I, inhibitory; E, expressor; D, drive) with medication. Each point represents the firing of one cell in the network. The blue (untreated) trace dips at the time of the seizure (arrow); anti-epileptic medication prevented this from happening, without affecting baseline dynamics of the network. Modified from Lytton and Omurtag (2007).

23.2 Parkinson's Disease

Parkinson's disease is one of several neurodegenerative disorders which affect a particular population of neurons whose degeneration deprives the rest of the brain of a needed projection or needed neuromodulator. In the case of PD, this population is the neurons of the substantia nigra pars compacta (SNc) in the brain stem. These neurons release the neurotransmitter dopamine and project strongly to the basal ganglia. Their degeneration results in reduction of the dopamine levels in the basal ganglia, producing a group of symptoms which are initially primarily motoric—movement problems. The disease then progresses to affect non-motoric brain functions as well. The major symptoms include difficulty initiating movements, slowed movement (bradykinesia) with concomitant slowed thought (bradyphrenia), increased muscle tone around the joints (rigidity), resting tremors, and difficulty coordinating bodily movements (postural instability).

The initial treatment of PD involves exogenous replacement of missing dopamine. This can be done by either providing a dopamine precursor (L-dopa) which gets converted into dopamine in the brain, or providing agonist drugs to activate dopamine receptors. Initially, this therapy produces improvement of several aspects of the disease, for example, reduced rigidity, faster spontaneous movements, and reduced tremor. Interestingly, there is sometimes an initial dramatic response to replacement, with the patient reporting a seemingly miraculous return to normal function. This is impressive since the original phasic release of the dopamine has been replaced by a continuous tonic dopamine "bath." Unfortunately, later on, the symptoms will start appearing again despite the treatment and then may be more severe than they otherwise would have been, perhaps because of downregulation of dopamine receptors (Hermanowicz, 2007). Such downregulation would be an example of homeostasis—maintenance of activity equilibrium in the face of change. In this case the abnormally high, continuous level of dopamine would reduce the sensitivity of the neurons to dopamine by reducing (downregulating) the number of dopamine receptors.

23.2.1 Anatomy and Function of Basal Ganglia

The basal ganglia consists of different nuclei and are divided anatomically into striatum, the major input portal to the basal ganglia, and globus pallidus, the output route. (See figure 23.3, and also chapter 22, "Integrative Functions of the Corticostriatal System.") The striatum receives inputs from multiple cortical areas and is further subdivided into caudate nucleus and putamen. In primates, the caudate nucleus receives cortical input from the prefrontal cortex while the putamen receives inputs from the somatosensory and motor cortices. The main cells in the striatum are GABAergic neurons—medium spiny projection neurons—that project to the globus pallidus interna (GPi) and substantia nigra pars reticulata (SNr) but not to SNc, the site of dopamine production. The GPi and SNr are main output pathways and also have GABAergic projection neurons. These areas convey signals from the striatum to the thalamus and thence back to cortex. This circuit therefore provides a cortico–striato–pallido–thalamo–cortical loop. Note that the primary projections pathways within and from striatum are GABAergic and therefore inhibitory; this differs from cortex and thalamus where the major projections are glutamatergic, excitatory projections. SNc and the neighboring ventral tegmental area (VTA) are the dopaminergic areas that provide projections to striatum (Gerfen and Bolam, 2010). An additional level of circuit complexity arises due to the existence of at least two major classes of striatal cells, D1 striatal cells and D2 striatal cells, which have two different types of dopamine receptors (D1 and D2) with very different cellular effects (Richfield et al., 1989).

The basal ganglia circuitry has been conceptualized as instantiating Go and No-go circuits.

GPi/SNr inhibits thalamus. Therefore, inhibition of GPi/SNr results in disinhibition of thalamus (Go signal). Stimulation of GPi/SNr results in inhibition of thalamus (No-go signal) (Chevalier and Deniau, 1990). So stimulation of Dl cells in striatum (which inhibits GPi/SNr; direct pathway) results in a Go signal for a *task* to be performed. Stimulation of D2 cells in the striatum (which disinhibits GPi/SNr through globus pallidus externa [GPe]; indirect pathway) results in a No-go signal: the *task* is less likely to be performed. Presumably, the No-go signal is not guaranteed to always override the Go signal generated. Since D2 receptors have higher affinity for dopamine than Dl receptors (Richfield et al., 1989), dopamine depletion in PD results in D2 receptors' being more active, which causes the indirect pathway (responsible for the No-go signal) to be more active.

The basal ganglia is also involved in reinforcement learning (RL). This is another place where modeling has been particularly helpful (see chapter 12 for an extended exposition) since learning theory is an important focus of computational neuroscience. RL takes place through variation in phasic release of dopamine. Phasic bursts of dopamine are related to receiving unexpected reward (positive feedback, which results in reinforcing the behavior). In contrast, phasic dips of dopamine are related to not receiving an expected reward (negative feedback, resulting in reduction of behavior). Bursts and dips follow positive and negative feedback based on prediction error. This is part of the reason why patients suffering from PD suffer from

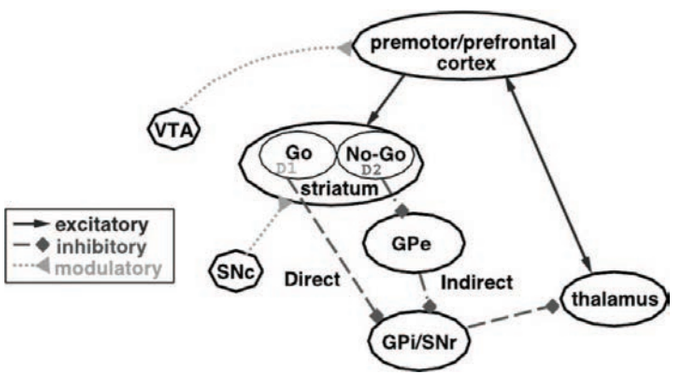

Figure 23.3 Schematic illustration for basal ganglia connections, showing the cortico–striato–pallido–thalamo–cortical loop. Premotor/prefrontal cortex projects to the striatum. D1 cells send inhibitory projections to globus pallidus interna (GPi)/substantia nigra pars reticulata (SNr) (direct pathway), while D2 cells send inhibitory projections to globus pallidus externa (GPe), which projects to GPi/SNr (indirect pathway). GPi/SNr then projects to the thalamus, which projects back to the cortex. Substantia nigra pars compacta (SNc) and ventral tegmental area (VTA) have modulatory dopaminergic projections to striatum; VTA also modulates cortex directly. From Frank (2005).

learning deficits and have impairment in tasks related to trial-by-trial error feedback.

Another way of viewing the basal ganglia is as a selection circuit and a control circuit, corresponding generally to the Go/No-go dichotomy mentioned above. GPi/SNr tonically inhibits thalamus. When a subset of GPi/SNr neurons themselves become inhibited by focused input from D1 striatal cells, activities mediated by that portion of the thalamus are allowed (figure 23.4). GPi/SNr neurons are under continuous stimulation by diffuse excitation from subthalamic nucleus (STN), and so those that are not inhibited from striatum continue to provide inhibition to these other portions of thalamus. This produces contrast between selected and non-selected neurons in the thalamus. In this way, focal activation of a group of D1 striatal cells by cortex selects certain circuits for ongoing activation. Meanwhile, inhibitory signals to GPi/SNr arise from the GPe, which receives inhibitory signals from D2 striatal cells (control circuit). This is, of course, a highly simplified model (Bevan et al., 1998; Nambu et al., 2002).

Given the complexity of basal ganglia circuitry, modeling approaches have been particularly valuable. As in other systems, we look for a relatively clear-cut task that requires the use of this system. In the case of basal ganglia, one such task is the initiation of Go and No-go signals. After initiation, these signals are sent to various brain circuits responsible for different brain functions: walk or not, switch from one task to another, think about one thing or another. This task also makes sense in terms of the pathology of PD, in that these patients

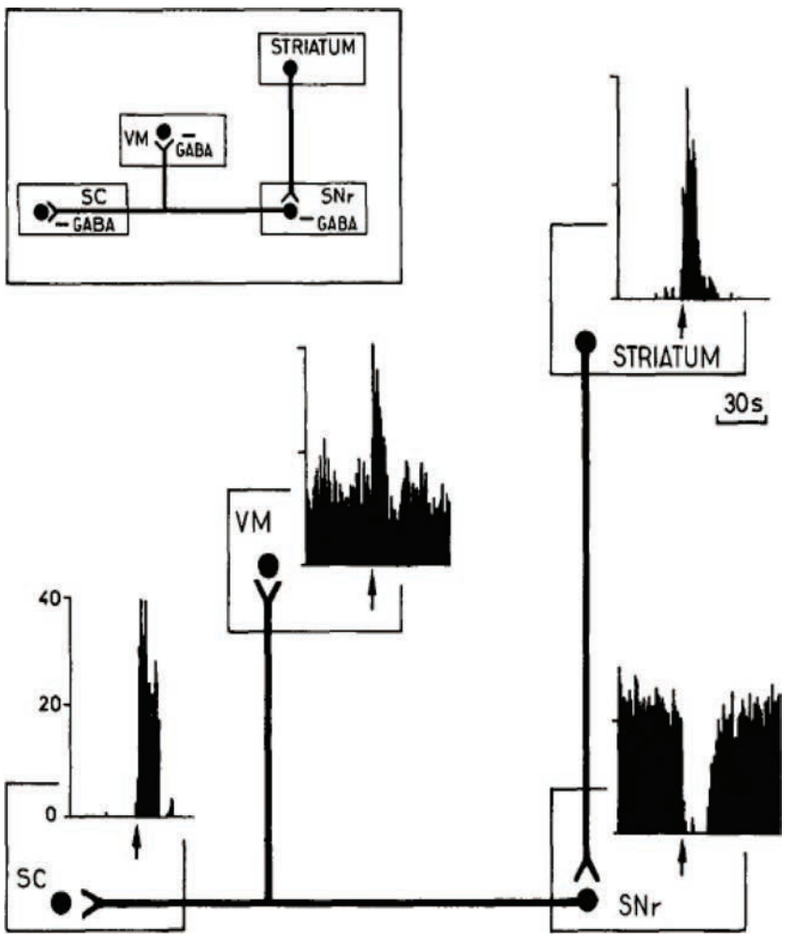

FIGURE 23.4 Disinhibition of thalamus following stimulation of striatum (time on *x*-axis, spikes per second on *y*-axis). In the upper right plot, the arrow shows applying glutamate to stimulate striatum. The arrows correspond to the same point in time in the four plots. The increase in firing in the striatum corresponds to reduction of firing in the substantia nigra pars reticulata (SNr), which results in increase in firing in the thalamus (VM, ventromedial nucleus of thalamus) and superior colliculus (SC) through disinhibition. This increase in firing would send an activation signal to the cortex. From Chevalier and Deniau (1990).

find it difficult to initiate movements or to abruptly stop (festination). It could also help in explaining the perseveration sometimes observed in these patients when they keep repeating certain phrases.

Similar to many clinical phenomena, PD crosses multiple spatial and temporal scales. As a disease process, PD starts at the cellular and molecular levels with degeneration of the neurons in the SNc, with the resultant reduction of dopamine levels at the basal ganglia. However, the symptoms appear at the behavioral level, in the form of problems in motoric functions and in learning. Treatment takes place at a molecular level, the level of dopamine receptors, while the improvement of symptoms takes place at a behavioral level. Computational neuroscience is needed to bridge these spatial and temporal scales.

23.2.2 Modeling the Role of Dopamine in Selection We give an example of an effort to explore the selection function of the basal ganglia circuitry and the role played by dopamine (Humphries et al., 2006). This study modeled five components of the basal ganglia circuitry: striatal D1 cells, striatal D2 cells, STN, globus pallidus (which represented GPe), and SNr (representing basal ganglia output). The leaky integrate-and-fire neurons within each of these structures were divided into three groups, corresponding to three different actions. Each group is connected to a corresponding group in each of the components, maintaining the topographic arrangement of fibers that is seen in the parallel loops that exist between striatum, GPe, GPi/SNr, thalamus, and cortex in the cortico–striato–pallido–thalamo–cortical circuit (figure 23.5)

Cortical input to the striatum (D1 and D2 cell populations) and STN was simulated using spike trains of different frequencies. This would correspond to saliency of a stimulus in real life, with the higher frequency representing a stimulus that has a higher salience. The stimulation protocol that was used to test action selection consisted of an input to group 1 at t = l second, followed by an input with a different frequency in group 2 at t = 2.5 seconds. The stimulation was terminated at 5 seconds. According to the action selection prediction, the basal ganglia model should be able to select a group at t = l, the beginning of the first stimulus. The model should then only switch the selection to the second group, presented at t = 2.5, in cases when the second group is more salient, represented as higher frequency firing in that group. Selection of a group was considered to have taken place when the firing rate of an SNr group dropped below a threshold. This was taken to be the case because, physiologically, reduced firing in one SNr population will disinhibit the corresponding

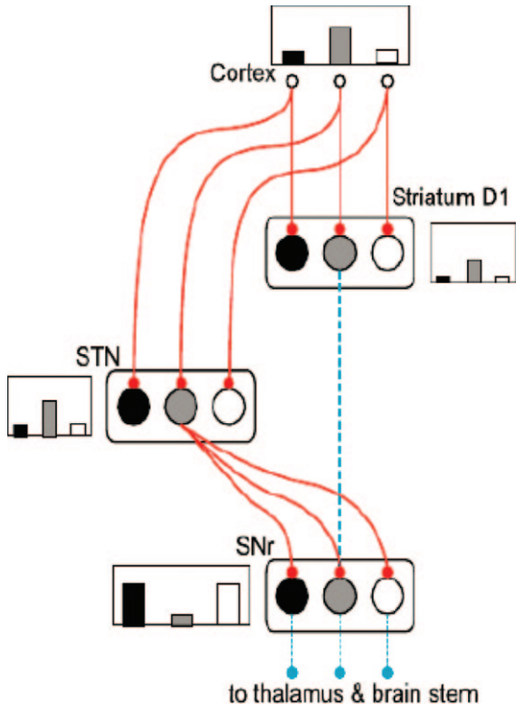

Figure 23.5 Groups of neurons in the selection circuit. The circuit responsible for selection of action in the model consists of the cortex, the D1 cells in striatum, subthalamic nucleus (STN), and substantia nigra pars reticulata (SNr). Each of those structures has three groups of neurons (black, gray, and white) corresponding to three different actions. Each group in each of the structures projects to the corresponding group (only connections of the gray population are shown in details), except for STN which projects diffusely (only the gray projections from STN are shown). Modified from Humphries et al. (2006).

population in thalamus, which will in turn stimulate the corresponding cortical population.

Different levels of simulated tonic dopamine on both D1 and D2 cells were used to simulate healthy basal ganglia circuitry, PD pathology, and PD with excess dopamine during excessive dopaminergic therapy. Dopamine's effect on synapses was modeled as follows:

$$I^{S}_{i\in\Omega S1} = (I^{ampa} + I^{nmda})(1+\lambda_{D1}), \qquad (23.4)$$

$$I^{S}_{i\in\Omega S2} = (I^{ampa} + I^{nmda})(1+\lambda_{D2}), \qquad (23.5)$$

where $I^{S}_{i\in\Omega S1}$ and $I^{S}_{i\in\Omega S2}$ are the currents in the soma of the i neuron that belongs to D1 ($\Omega S1$) or D2 ($\Omega S2$) cell populations in the striatum. I^{ampa} and I^{nmda} are the currents provided by excitatory synapses, mediated by AMPA and NMDA glutamatergic receptors, respectively. These receptors are involved in the classical driving of synapses, contrasted with neuromodulatory synapses

such as those for dopamine, which depend on input from the cortex. λ_{D1} and λ_{D2} are the tonic levels of dopamine on D1 and D2 receptors, respectively, ranging from zero to 1. To simulate physiological amounts of dopamine, both λ_{D1} and λ_{D2} were set to 0.3. To simulate PD, values were set to zero. They were set to 1 for the case of excess dopamine under the effect of excess dopamine therapy. From equations 23.4 and 23.5, this variation will result in changes in the synaptic current. So, in comparison to the physiological state, in the case of PD, the activating synaptic currents from the cortex (carrying the signal), would reduce firing of D1 population and increase firing of D2 population. Both of these changes would disinhibit SNr cells (which receives GABAergic projections from Dl and GPe populations), increasing their firing and so the groups are considered not selected. In the opposite case, with excess dopamine (with λ_{D1} and λ_{D2} set to 1), this will result in increased excitatory synaptic current to the D1 cells and reduction in those currents to the D2 cells. Both these changes will result in reduction of SNr firing (which is considered as selection).

The physiological model was able to exhibit action (group) selection (blue circles in figure 23.6A): the SNr group was selected when the first input was given, and then switched to the other group when the more significant stimulus was introduced (the stimulus with the higher frequency). With low levels of dopamine (simulating PD), neither signal selection nor switching took place (figure 23.6B). The firing rate of the corresponding groups in SNr dropped slightly, but not sufficiently to indicate group selection. With excess dopamine (to simulate what happens with dopamine replacement therapy or dopamine agonists), switching becomes rare as competition between inputs results in selection of *both* first and second groups. With the introduction of the first stimulus, the group is selected. Then with introduction of the second stimulus through a second group, the second group is also selected, with no de-selection of the first one (green diamonds in figure 23.6C).

The above results points to the nonlinear mode of action of dopamine. Reduction of dopamine (as in PD) would result in dysfunction because of limited ability to select responses to stimuli. High levels of dopamine (like what happens with overtreatment using L-dopa or dopamine agonists) would also result in dysfunction because of inability to respond to a more salient stimulus presented after a less salient stimulus.

Here we have looked at some effects of dopamine on synaptic activation. Another related effect is the

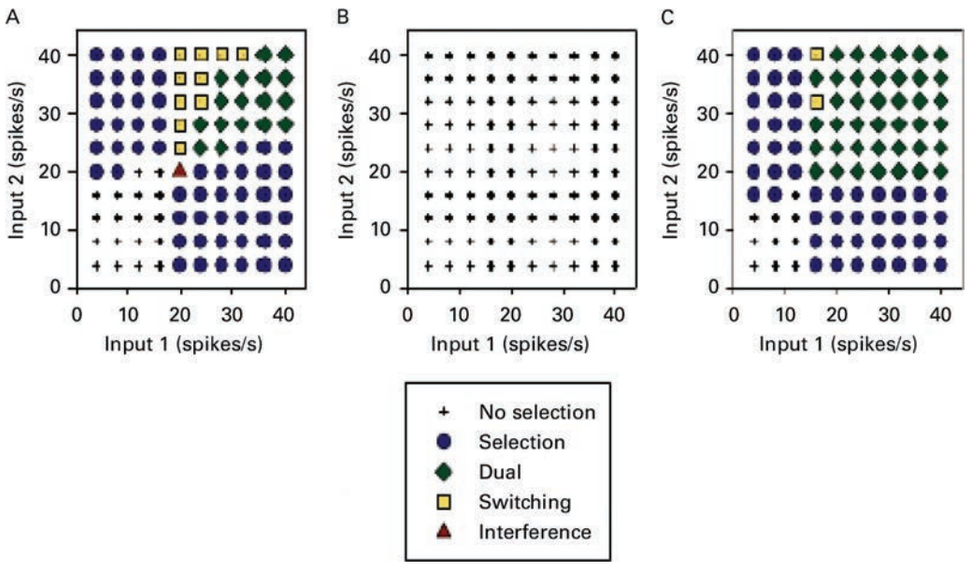

FIGURE 23.6 The grids A, B, and C represents the behaviors of the models under normal, low, and high dopamine levels, respectively. Each point in the grid represents a simulation. The *x*-axis and *y*-axis represents the spiking in channels 1 and 2, respectively. For each of the simulations, the model is presented with a stimulus along one channel, then with another more salient stimulus along the other channel. As seen in grid A (normal dopamine level), the stimulus with higher salience is selected (blue circles in the bottom-right and top-left corners of the grid). With low dopamine levels (as in PD, grid B), there is lack of selection of either group of neurons (crosses in the plot denoting "no selection"). With higher dopamine levels (grid C), there is competition, and switching takes place (yellow squares). With higher spiking rates, both channels are selected (dual selection, green diamonds). So, with high levels of dopamine, there is less switching and more dual representations of the channels. Modified from Humphries et al. (2006).

enhancement of synapses as part of RL, which we will explore in the next section.

23.2.3 Modeling Effects of Tonic and Phasic Dopamine Another computer model investigated the effects of dopamine depletion and repletion on both tonic and phasic dopamine inputs (Frank, 2005). The model consisted of elements representing cue input, striatum, GPe, GPi (as the output port), thalamus, premotor cortex (PMC, which projects to the output layer), and SNc (which supplied dopamine input to the striatum). These elements consist of units that behave like point neurons, with rate coding. The striatum had a Go and a No-go column for each of two possible responses, giving a total of four columns of activation "units." Each of the Go columns projected to GPi. Each of the No-go columns projected to GPe, which then projected to GPi. This way, based on competition in the level of activity of the units in each column in the striatum, GPi ended up with a level of activity which influenced the thalamic units in an inhibitory fashion. Thalamic units then projected to PMC units, which projected to the output element.

The model was used on two tasks. In the first, the network was presented with different cues in different combinations. Each cue had a probability to predict either "rain" or "sun." There were two learning phases. One phase was dependent on tonic dopamine stimulation from the SNc (the "minus" phase). During this phase, the network was presented with cues, and based on a given cue and the synaptic weights, a response was picked up. No feedback was given about whether the response was correct or not. During the second phase ("plus" phase), feedback was provided based on the response. A correct response resulted in an increase of dopamine stimulation, a dopamine "burst." This resulted in an enhancement of the Go signal and a reduction in the No-go signal, encouraging the network to select that response when presented with a similar set of cues next time. An incorrect response resulted in a decrease in dopamine stimulation ("dip"), reducing the Go signal and enhancing the No-go signal. The feedback modified the weights of the synapses from the input layer and from the PMC layer onto the striatum. Through this learning, the activation of the correct units of striatum was achieved.

The second task was a *probabilistic reversal task*. The model was presented with one of two cues and learned to associate one of two responses with each cue. Reversal then took place, and the network had to learn to associate the same cue with the opposite response (i.e., unlearn the previous learning).

In order to simulate PD pathology, three out of the four units representing SNc were silenced to form a "PD network." This resulted in a lower tonic level of dopamine, and also a smaller difference between the dopamine burst and dip.

Intact and PD networks were given both tasks. PD networks showed more errors in both tasks in comparison to the intact networks. To simulate the medicated state, a network with higher dopamine input during the tonic, burst, and dip phases was modeled. The effect of medication was compared on the network in the probabilistic reversal task. In comparison to the intact network, the medicated network was more prone to errors in the probabilistic reversal task during the part that required reversal of acquired learning. This happened because the high levels of dopamine suppressed the No-go units and so impaired the network's ability to learn No-go representations during negative feedback, important to allow for learning reversal. This model was able to replicate the phenomenon of patients suffering from PD being prone to different types of ~~error~~, even when medicated.

As discussed, modeling can help in evaluating the effect that various levels of neurotransmitter can have on basal ganglia circuitry. Future modeling efforts will begin to look at the progression of PD by considering how alterations in dopamine levels over time will alter the expression of disease.

23.3 Stroke

23.3.1 Pathophysiology and Dynamics of Stroke The brain receives its blood supply through a network of blood vessels which supplies the brain in a pattern unrelated to the functions of the supplied areas. Therefore, strokes can produce peculiar patterns of deficit through effects on multiple brain areas related by proximity but not by functional interconnection. After the blood supply to a brain region stops, neurons suffer from reduction of oxygen and glucose supply. They become ischemic. If this continues for a prolonged period of time, the neurons start to die. A stroke develops when neurons die following the cessation or reduction of blood supply to a brain region. Note that such a region is determined by the blood supply, and has no relation to, for example, neuroanatomical regions in the sense of Brodmann areas.

The area surrounding the region where the blood supply is reduced, but where neurons have not yet died, is called the penumbra. The neurons within the penumbra show reduced metabolic and neural function and are sensitive to further insult either through further reduction in their metabolic supplies or through

additional excessive excitation. This excessive excitation, termed excitotoxicity, can occur either through synaptic activation or through nonspecific stimulation of glutamate receptors by glutamate released into the extracellular space from other damaged cells.

Cortical representations of different body regions are dynamic. They change in response to alterations of received stimulus characteristics. For example, excessive stimulation of a body region will result in expansion of the sensory cortical area representing that body part (Buonomano and Merzenich, 1998). (See chapter 13, "Neural Maps: Their Function and Development.") In contrast, decreased stimulation of a body part—for example, by surgical removal of a finger—results in diminishing the size of the sensory cortical region representing the finger (Kaas et al., 1983). Following a stroke, changes occur in the other direction: the sensory organ is present, but the sensory cortical region representing that sensory organ is now missing. In order to understand changes following stroke, it is useful to think in terms of receptive fields (RFs) and projective fields. The RF of a neuron is the area from where the neuron is *receiving* its input (an area of a finger, in the above example, which will activate a particular neuron). A projective field is the set of neurons activated when a single location is stimulated, that is, the set of neurons onto which a particular location *projects*.

It is hypothesized that changes in the RFs of surviving cells may play a role in recovery following stroke: the function of the cells that are missing may be replaced in part by local cells with similar or overlapping RFs. The alternative, but not mutually exclusive, hypothesis is that other remote areas of the brain take over functions once handled by the ischemic area. The MT (middle temporal cortex, or V5) region which is involved in representing the motion of different targets in the visual field represents an interesting example. A lesion in the MT region in monkeys does not impair the monkey's ability to see stationary targets but does impair its ability to track moving objects when they are present in the area of the visual field represented by the lesioned part (Wurtz et al., 1990). Following a lesion to the MT cortex of a monkey, changes take place immediately within the RFs of remaining cells surrounding the ablated MT area. These surrounding cells would be comparable to the cells of the penumbra in a stroke. The changes occurring include both expansion and contraction as well as shifting of RFs. Expansion is often asymmetrical, with a tendency to expand primarily toward the lesion.

23.3.2 Modeling RFs Changes To investigate changes in RFs, a model was developed that used a one-layer recurrent model of MT which received convergent inputs from a receptive layer representing lower visual areas such as V1 (Lytton et al., 1999). The MT layer had lateral connections, in the form of near excitatory and far inhibitory connections (a "Mexican hat" distribution of connections, but with no self-excitation; figure 23.7).

Simulations on this network demonstrated that a process of unmasking could explain expansion and contraction of the RFs (figure 23.8). Cells in the network provided near excitatory, and far inhibitory, lateral inputs. After ablation, these influences were lost, resulting in loss of both the local excitatory and the distal inhibitory connections that had originated from the ablated region. The loss of nearby excitatory cells had a minimal effect. However, the loss of the more distant inhibitory connections resulted in substantial increased activation *(unmasking)* such that receptive inputs that were previously unable to activate a given MT unit could now do so, having less inhibition to counter. This resulted in expansion of the RF. A secondary consequence of this loss of inhibition was due to the disinhibition of inhibitory cells. This secondary effect resulted in contraction of the RFs for the principal cells that now received augmented inhibition. Inputs that previously would have stimulated these cells to threshold were no longer capable of doing so. Such expansion and contraction in the RFs represent an expanding wave of dynamical consequences resulting from the loss of projections from the lost neurons.

While the simulation was able to replicate both expansion and contraction of RFs, the contractions seen were much less than those found in the experimental animal model. This failure meant that there was a missing element, a missing piece in the model. This

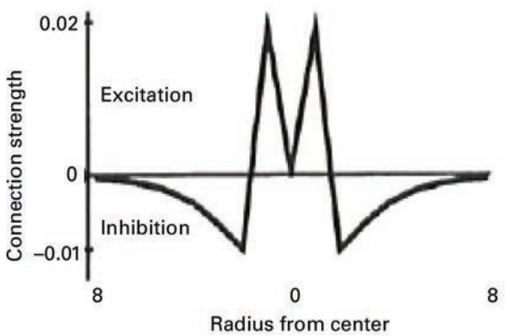

Figure 23.7 Lateral connections within the layer representing the middle temporal area. There are no self–self connections (connection strength = 0, at radius = 0). There are nearby excitatory connections and far inhibitory connections. From Lytton et al. (1999).

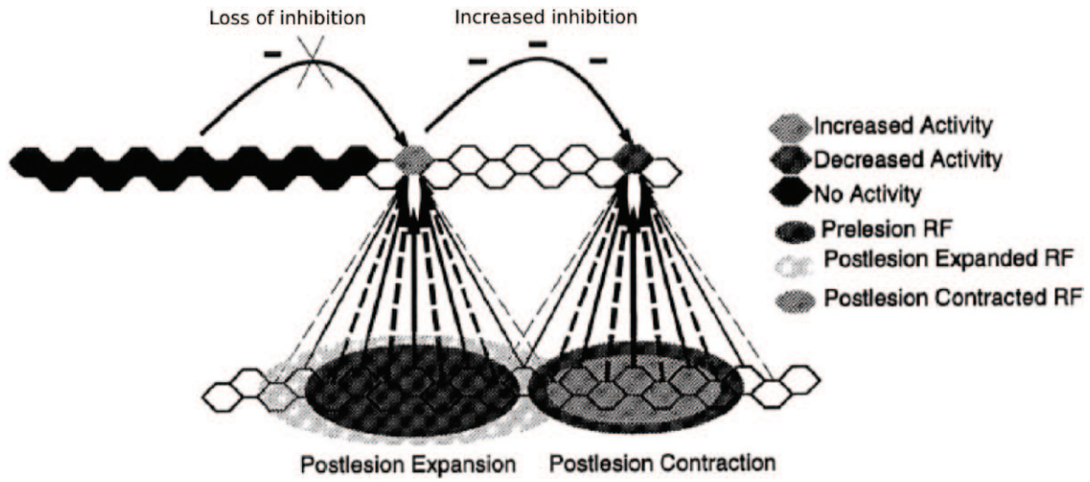

FIGURE 23.8 Unmasking can explain expansion and contraction of receptive fields (RFs) post-lesion. The top layer is middle temporal cortex (MT) while the lower one is Vl. Inputs from Vl activate MT. In the MT layer, the left half is ablated. This results in loss of inhibition onto the region in the middle (light gray hexagon in top layer). This disinhibition reduces the activity in the right-most dark gray hexagon. Since the middle light gray hexagon is no longer inhibited, it can be activated by previously subthreshold input from wider regions of Vl (RF expansion in the bottom layer, on the left). Similarly, since the dark gray hexagon now receives more lateral inhibition, its threshold has increased and so will respond to narrower regions of Vl that can provide suprathreshold input (RF contraction in the bottom layer, on the right). From Lytton et al. (1999).

problem highlights the important role of failure (falsifiability) in modeling—the inability to explain some aspect of reality spurs the experimental search for additional critical facts about the system. This also highlights a contrast between simulation modeling and traditional closed-form physics modeling. Falsification in simulation generally requires that a model be augmented, whereas in closed-form modeling it may require that the model be entirely abandoned.

When the histology of the ischemic regions was looked at more carefully, it was found that there is reduced expression of $GABA_A$ receptors in the vicinity of stroke (Schiene et al., 1996), as well as increased excitability in these regions (Neumann-Haefelin et al., 1995). This suggests the presence of a halo of disinhibition around the ablated area. This is consistent with the inhibitory interneurons being more sensitive to ischemia, and so more of them are affected. The presence of this halo suggested that the penumbra region would show differential effects on the various kinds of cells found in the region.

When this halo was included in the model, it resulted in augmentation of both expansion and contraction of the RFs. Excitatory cells in the disinhibition halo were excitable by the relatively weak stimulation coming from distantly converging inputs resulting in expansion of their RFs. Also, the excessive activity in these cells produced increased inhibition in the inhibitory ring (the cells receiving the far inhibitory input), making it more difficult for units from the input layer to stimulate these units. This now resulted in more pronounced contractions, more similar to those seen experimentally. The mechanism of expansion and contraction of RF was the same in the simple model and the model with the disinhibited halo. However, the halo augmented the effects of each mechanism.

While the changes described in the model occurred immediately, cortical networks are dynamic on different timescales. This suggests that overall RF changes would likely take place in two phases. The first phase involves the immediate changes in neuronal dynamics described in this model which were the immediate consequence of cell death, with loss of the various excitatory and inhibitory connections on neighboring cells. During the second phase, synaptic plasticity changes would take place through changes in the synaptic weights among the surviving neurons. These changes will follow a pattern that would be determined by the new dynamics which resulted from the first phase. Naturally, synaptic plasticity changes will also result in changes in neuronal dynamics, closing the loop between these two interacting processes. Dynamic changes give rise to plasticity, and plasticity consists of structural changes that give rise to dynamic changes. Separating them into two phases is nonetheless justified by the vastly different time constants for each of them. While the neural dynamic

changes take place over the course of milliseconds, the synaptic plasticity changes take place over the course of hours to days.

Perception depends on neural activity, and stroke results in alterations in encoding. If the decoding strategy leading to behavior were to remain unchanged, function would suffer. For this reason, full behavioral recovery will require changes in decoding strategy that match the alterations in encoding (see, e.g., Nudo, 2007).

To explore the effect of ablation on neural coding, the model was expanded so that input was represented as a stimulus with attributes of location, direction of motion, and speed. Also, the MT units (which respond to movements, with the attributes of direction and speed) were replaced with a set of units, each of which was assigned a preferred direction and speed. A winner-take-all algorithm was used to interpret neural activity. (Other algorithms that could have been used to determine the characteristics of the stimulus are vector sum or vector average.)

Animal stroke models and clinical experience suggest that a stroke in the MT visual area will produce a behavioral effect. In this case the effect would be a motion scotoma in the visual field: an area of the visual field with a perceptual deficit for moving target leading to underestimation of the speed of the target. This can be measured through measuring the lag of the eye movements, or the reduction in pursuit speed during following the target with the eyes. The model was able to reproduce this effect, producing underestimation of object speed within the region that corresponded to the ablated area.

Based on the model discussed, it is suggested that the expansion of the RF following ablation allows post-lesion stimuli to be misprocessed (as evidenced by inappropriate post-lesion behavior) rather than not processed at all. In the absence of these expansions, a portion of visual space would lose its cortical representation entirely because it would not fall in the RFs of any live neurons. Immediate RF expansion might produce a "Band-Aid effect" that is important both to immediate preservation of function and to the eventual shift and spread of RFs to fill the gap after cortical reorganization.

Hebbian synaptic plasticity suggests how physical therapies might improve functional recovery following stroke. According to this mechanism, synapses become strengthened when there is coincident activation of the presynaptic and postsynaptic neurons, and they get weakened when the activation of both neurons is not coincident. The model showed that stroke is likely to produce increased activation of a set of cortical neurons, which will then lead to increased synaptic strength with other neurons that are active. By purposefully activating specific pathways either by peripheral input (through physiotherapy) or cortical stimulation, one could produce desired synaptic connectivity to compensate for lost pathways. Presumably, specific patterns of exercises currently used in physical therapy determine synaptic reorganization in the brain.

Understanding the events underlying the immediate and the synaptic plasticity phases of changes following stroke points toward pharmacological and nonpharmacological interventions (e.g., physiotherapy) to minimize neuronal death after stroke (minimizing deficit) and promote synaptic plasticity (improving recovery). For example, it may be desirable to delay the onset of cortical reorganization to prevent formation of spurious connections caused by overexcited neurons of the ischemic penumbra. Or, an agent that can pharmacologically erase long-term potentiation, such as zeta inhibitory protein (Shema et al., 2007), might be used to allow cortical reorganization to occur during a period of intensive physical therapy which has been postponed till after medical therapy and recovery occur.

Computer models for the recovery process which takes place with physiotherapy provide clinical predictions. Subjects with a stroke affecting one hand will tend not to use it, and therapy may constrain the good hand to encourage the patient's use of the impaired hand. Han and colleagues (Han et al., 2008; Schweighofer et al., 2009) developed a model of the recovery process which predicted a functional threshold, beyond which improved use of the affected limb would lead to greater spontaneous use. This would then provide a virtuous circle which would provide continued improvement without the need for further explicit rehabilitation strategies.

They modeled motor cortex in both hemispheres and produced a stroke on one side. Neural reorganization in the motor cortex was modeled to include supervised, unsupervised, and reinforcement learning. The existence of the threshold could be explained by taking into account the complex interaction of learning dynamics across all three types of learning that were simulated. A subsequent study determined such a functional threshold clinically (Schweighofer et al., 2009). An important result of comparing model with clinical reality was that not all patients showed the same effects. Overall, the threshold could be shown in the group, with most of the patients improving above that threshold. Ideally, more detailed modeling could be used clinically to assess threshold for individual patients.

Modeling of the effect of ablation and stroke allowed the exploration of the dynamical changes that happen

afterward, which play a role in recovery. We will now turn to investigating brain oscillations, their role in schizophrenia, and how modeling them can aid in pointing to targets for therapy.

23.4 Schizophrenia

23.4.1 Schizophrenia and Oscillations We have left schizophrenia for last as it remains one of the most puzzling of brain diseases and also one of the most challenging for modeling since it primarily affects thought processing. While the prior diseases are considered neurological, schizophrenia is considered psychiatric. This distinction reflects both historical and practical issues. Historically, schizophrenia was considered a disease of the mind rather than a disease of the brain. Hence, it was thought that it was a disease that could be cured by somehow replacing wrong thinking with right thinking, comparable to classical religious views of the origins of thought and behavior. Now it has become clear that schizophrenia is in fact a brain disease and that any treatment will have to address problems in the brain as well as trying to ameliorate learned behaviors. However, since psychiatry is considered to deal more with symptoms of the mind, schizophrenia is still treated by psychiatrists and in psychiatric settings. The dichotomy between neurology and psychiatry remains important logistically.

Patients with schizophrenia present with symptoms that belong to one of three domains: positive, cognitive, and negative symptoms. "Positive" symptoms include hallucinations (usually auditory, but they could also be visual), delusions (false fixed beliefs that the patient holds strongly, which are not shared by others of the same culture), and disorganized thought processes (where the forms of thought and speech become disrupted so that it is difficult to understand what the patient is trying to say or communicate). Cognitive symptoms include deficits of working memory (patients have difficulty holding information that is important to solve a task at hand, e.g., preparing a grocery list). Negative symptoms include lack of motivation and social isolation. Current available medications (antipsychotics) can control positive symptoms. However, the effects on improving cognitive and negative symptoms are still limited.

Different patients will manifest different combinations of symptoms. It is now accepted that both etiology (the cause, the why) and pathophysiology (the mechanism, the how) in schizophrenia are multifactorial. Etiologies include genetic susceptibility, intrauterine exposure to infections, and stressful life situations. No one of these factors is enough by itself to cause schizophrenia, but it is the cumulative effect of these factors that finally causes schizophrenia to occur. Progress in understanding and treating schizophrenia has been slow, in large part because of this multifactorial nature. No one set of studies holds the key to understanding schizophrenia, and no one researcher is likely to master all of the disparate threads that need to be pulled together. Computer modeling has been proposed as a technique that will eventually permit us to master this complexity.

Here, we focus on pathogenesis and look at one set of theories that has strong evidence from animal studies and neuropsychological testing: cognitive coordination (Phillips and Silverstein, 2003). According to cognitive coordination theory, different regions and networks of the brain are able to perform their function through coordinating their activities within themselves and between each other. Symptoms of schizophrenia arise because of failure of the coordination between brain networks (cognitive discoordination).

23.4.2 Schizophrenia and Oscillations Oscillations, ubiquitous in the brain, have been hypothesized to provide the neural coordination that underlies cognitive coordination (Bressler and Kelso, 2001). Oscillations within and between different brain networks may synchronize the firing of neuronal networks that are functionally related. Such synchronization has been hypothesized to underlie the "binding" of various attributes of an object to create the conscious perception of a unified object. In the context of schizophrenia, this would then suggest anomalies in binding that could lead to the cognitive and perceptual disorders associated with this disease.

Ketamine, one of the chemical relatives to PCP (phencyclidine, or angel dust) is an NMDA receptor (NMDAR) antagonist that is used as an anesthetic. As we mentioned above, NMDA is one of the glutamate receptors responsible for excitatory activation of the postsynaptic cell. When ketamine, in subanesthetic dose, is given to nonpsychotic human subjects (those who do not suffer from schizophrenia or related disorders), they start experiencing hallucinations, delusions, and thought process disturbances. When ketamine is given to patients with history of schizophrenia, it exacerbates and worsens their symptoms. Ketamine also produces changes in brain oscillations. In mice, these changes are an increase in the power of the gamma oscillations (30–100 Hz) and a decrease in the power of theta oscillations (3–12 Hz) (Lazarewicz et al., 2010). In humans, EEG changes have been recorded in healthy volunteers under subanesthetic doses of ketamine. The changes were increased power of

gamma-band oscillations (40–85 Hz), and decrease in the power of delta-band oscillations (1–5 Hz) (Hong et al., 2009). Psychotic symptoms were found to be associated with similar changes in EEG power spectra (Uhlhaas and Singer, 2010). Based on this, treatment with subanesthetic doses of ketamine is used to produce an animal model for schizophrenia (or psychosis in general). The change in the power of different frequency bands could be one of the mechanisms responsible for generation of psychotic symptoms.

23.4.3 Modeling Changes in Oscillations Hippocampus and frontal cortex are two areas primarily affected in schizophrenia. Postmortem brain biopsies from patients who suffered from schizophrenia showed changes in hippocampal cytoarchitecture (Harrison, 2004). To investigate how ketamine produces the observed changes in the power spectrum, a neural-level model of hippocampal circuitry was developed, consisting of 800 pyramidal neurons, 200 inhibitory fast-spiking basket cells, and 200 inhibitory slow-spiking oriens-lacunosum moleculare (OLM) cells. Theta drive from medial septum (MS) was simulated by providing periodic inhibitory input to OLM and basket cells. The connectivity of the network is shown schematically in figure 23.9. (See chapter 4 for other models of "Neural Rhythms.")

Oscillations within the model were generated as pyramidal cells drove OLM and basket cells via both AMPA (short) and NMDA (longer) receptor activation. The OLM cells, in turn, inhibited the distal dendrites of pyramidal cells, while the basket cells inhibited the soma of pyramidal cells. Compared to the fast changes in the membrane potential of pyramidal somata caused by basket cells, dendritic filtering gave the OLM inputs longer time constants, allowing them to modulate pyramidal activity with a slower time course. Gamma generation has been grossly dichotomized as being due to interneuron network gamma (ING) or pyramidal interneuron network gamma (PING) (See chapter 4, "Neural Rhythms."). ING appeared to be the major gamma driver at the theta nadir (figure 23.10C), when pyramidal cell population activation was minimal (figure 23.10A). By contrast, during the theta upswing, gamma activity appeared to primarily emerge as a PING interplay, the pyramidal cells driving the basket cells which then coordinated population pyramidal cell activity through near-simultaneous basket cell inhibitory postsynaptic potentials on pyramidal cell somata.

Basket cells were entrained to theta at two levels: directly by the MS inputs and indirectly via the periodic firing of the OLM-disinhibited pyramidal cells. The basket cells then provided feedback onto pyramidal cells that augmented their theta response. Removal of the basket cell population greatly reduced theta strength, demonstrating that basket cells contributed strongly to theta, as well as to gamma.

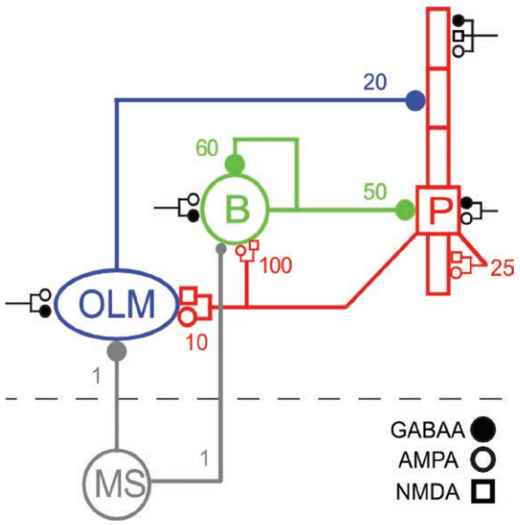

Figure 23.9 Schematic representation of the network representing the CA3 region of hippocampus. The network consists of 800 pyramidal neurons (P), 200 oriens-lacunosum moleculare inhibitory interneurons (OLM), and 200 basket cells (B). The numbers near the synapses represent convergence ratios, that is, number of inputs for an individual synapse: $GABA_A$ receptors (filled circles), AMPA receptors (open circles), NMDA receptors (open squares). External stimulation from other areas was modeled by synaptic bombardment (synapses with truncated lines). Externally generated theta oscillations from the medial septum (MS) were imposed on OLM and basket cells. From Neymotin et al. (2011).

Single-cell voltage traces reflected the dominant frequencies of basket cells and pyramidal cells. Individual OLM cells showed periodic firing on portions of the theta cycles after the recovery from MS inputs. The basket cell population fired at gamma frequency, but individual cells would only follow for 3–4 cycles at a time, and only at peak theta (figure 23.10D).

Ketamine blocks NMDA receptors. In the model, NMDA receptors are located on four locations: OLM soma, basket soma, pyramidal basal dendrite, and pyramidal apical dendrite. To simulate the blocking by ketamine at a particular site, conductance of NMDAR was set to zero at that site. Turning off all the NMDA synapses in the model reduced activity in all cell types, resulting in significant reduction in power for both theta and gamma. This did not match the experimental data (gamma up, theta down). Because different NMDA receptor subtypes that are expressed on different cell

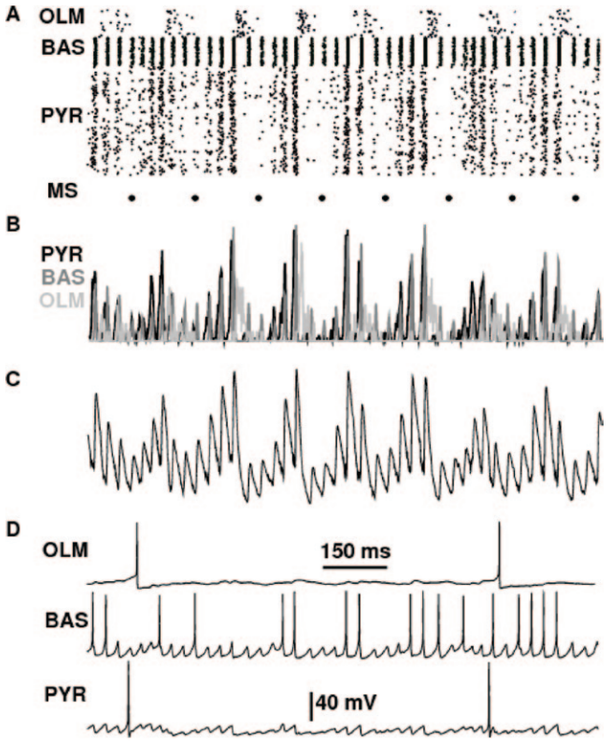

Figure 23.10 Network activity during baseline simulation. Network raster plot (A) shows the times of spikes in each cell organized into the three different cell populations—each dot on the raster is a single spike in a single cell. The periodic drive from medial septum (MS) is also shown. Spike densities (B) summarize the amount of spiking in each population over time by smoothing over the spikes in the raster plot (calculated using 1-ms bins and smoothing with 3-ms triangle filter). Local field potential (LFP; C) demonstrates the overall contribution of the pyramidal cells (PYR) as they would be seen by an electrode put into the brain. The single cell voltage traces (D) show the pattern of spikes and postsynaptic potentials (little bumps between spikes) for a representative cell for each of the three populations. Note that the fast frequency of activity seen in the LFP is an emergent population phenomenon based on many pyramidal cells firing together, despite each pyramidal cell firing infrequently. OLM, oriens-lacunosum moleculare cells. From Neymotin et al. (2011).

types have different sensitivity to NMDA-receptor antagonists (Bresink et al., 1995), it was hypothesized that the discrepancy might be due to different effects of ketamine on the different cell types. There were 16 combinations for blocking NMDAR on different sites. Changes in theta (3–12 Hz) and gamma (30–100 Hz) power were compared between the baseline and each of the combinations. Out of the 16 different combinations of NMDAR switched off, combinations that involved NMDAR being off at OLM cells replicated the experimental findings (Lazarewicz et al., 2010).

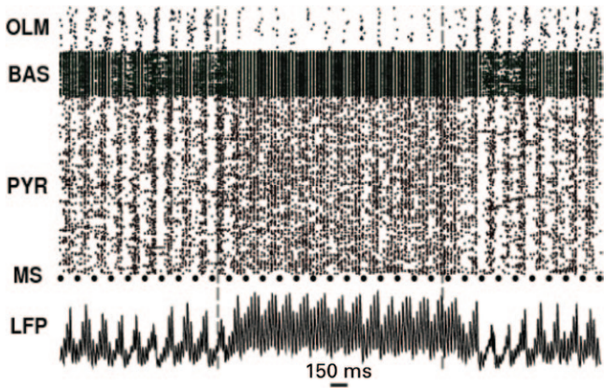

Figure 23.11 Raster plot (top) and local field potential (LFP) (bottom) showing baseline, ketamine wash-in, and wash-out from a single simulation. Vertical dotted lines mark times of ketamine wash-in and wash-out. During the period when ketamine is present, there is a great increase in the strength of fast (gamma) activity and a decrease in the strength of the slow (theta) activity. OLM, oriens-lacunosum moleculare cells; PYR, pyramidal cells; MS, medial septum. From Neymotin et al. (2011).

Therefore, it could be predicted that the experimental effect of ketamine is based on primary blockage at NMDA receptors on the OLM cells (figure 23.11).

These simulations suggested a sequence of pathophysiological alterations that led from a reduction in activity at a particular receptor to spectral changes at the network level. In order to restore the physiological power spectra of oscillations, a selective current injection into the OLM cell population was used, which recovered the control oscillations by direct opposition at the primary pathological focus. Here a tonic activation was used to replace a missing periodic effect, suggestive of the situation in PD where tonic dopamine replaces the phasic release that has been lost. Such a prediction points to the role computational neuroscience can play in pointing out possible mechanisms of action for new treatments even in a complex illness such as schizophrenia.

23.5 Summary and Conclusions

In this chapter, we have discussed four major brain diseases. We have focused on these diseases since this is where most of the modeling has been done. These diseases also represent something of a cross-section of the types of problems that can affect the brain. Epilepsy, for example, is the prototypical dynamical disease. A variety of insults or abnormalities, at different levels of organization, can result in dynamical perturbations that result in common symptomatic forms. Hence the

disease *is* the abnormal dynamics rather than being specific to one or the other of the possible causes. It is hypothesized that schizophrenia may represent a similar case, where multiple causes and levels of causation end up in a final common pathway of impaired neuronal dynamics, with the various manifestations being explained by the various circuits affected.

In epilepsy, there are multiple causes that converge on a relatively small set of manifestations. In PD, a single major disturbance diverges to produce several dynamical manifestations. For example, tremor and rigidity are not obviously related, an augmenting of movement contrasted with a decrementing. However, we are beginning to understand how this manifestation divergence might occur as expressions of underlying dynamical disturbances producing seemingly discrepant manifestations.

By contrast with the others, stroke is an ablative rather than a primarily dynamical disease and may have diverse loci, with varied effects accordingly. This ablation is imposed upon the brain, and the brain must react to it through alterations in activity that allow it to continue functioning at various levels. Although these alterations are also dynamical, it is reasonable to consider handling the pathology and responses to pathology as a series of snapshots at different points in time rather than necessarily following the dynamics in detail.

Because the brain is such a complex organ, with many underlying complex subsystems, its pathologies would also be expected to be extraordinarily complex and resistant to generalization. Thus, the presence of symptoms and signs that can be lumped together as a specific brain disease may be regarded as something of a surprise. However, the ways in which these symptoms and signs fit remains a major puzzle, a puzzle which we can hope to pull apart and then put back together using computational neuroscience. Nowhere is this puzzle more apparent than in schizophrenia, where bizarre ideas reflect thought disorders. Putting this shattered cognition back together again remains a far-off goal to which computational neuroscience can contribute, perhaps by yielding novel predictions that support the fitting of neural activity patterns back together through hitherto unexpected kinds of treatments.

REFERENCES

Bevan, M. D., Booth, P. A., Eaton, S. A., & Bolam, J. P. (1998). Selective innervation of neostriatal interneurons by a subclass of neuron in the globus pallidus of the rat. *Journal of Neuroscience*, *18*(22), 9438–9452.

Bresink, I., Danysz, W., Parsons, C., & Mutschler, E. (1995). Different binding affinities of NMDA receptor channel blockers in various brain regions—Indication of NMDA receptor heterogeneity. *Neuropharmacology*, *34*(5), 533–540.

Bressler, S. L., & Kelso, J. (2001). Cortical coordination dynamics and cognition. *Trends in Cognitive Sciences*, *5*(1), 26–36.

Buonomano, D. V., & Merzenich, M. M. (1998). Cortical plasticity: From synapses to maps. *Annual Review of Neuroscience*, *21*(1), 149–186.

Chevalier, G., & Deniau, J. (1990). Disinhibition as a basic process in the expression of striatal functions. *Trends in Neurosciences*, *13*(7), 277–280.

Frank, M. (2005). Dynamic dopamine modulation in the basal ganglia: A neurocomputational account of cognitive deficits in medicated and nonmedicated parkinsonism. *Journal of Cognitive Neuroscience*, *17*(1), 51–72.

Gerfen, C., & Bolam, J. (2010). The neuroanatomical organization of the basal ganglia. In H. Steiner & K. Tseng (Eds.), *Handbook of Basal Ganglia Structure and Function: A Decade of Progress* (Vol. 20). Access online via Elsevier.

Glass, L., & Mackey, M. (1988). *From Clocks to Chaos: The Rhythms of Life*. Princeton, NJ: Princeton University Press.

Han, C., Arbib, M., & Schweighofer, N. (2008). Stroke rehabilitation reaches a threshold. *PLoS Computational Biology*, *4*(8), e1000133.

Harrison, P. (2004). The hippocampus in schizophrenia: A review of the neuropathological evidence and its pathophysiological implications. *Psychopharmacology*, *174*(1), 151–162.

Hermanowicz, N. (2007). Drug therapy for Parkinson's disease. *Seminars in Neurology*, *27*, 97–105.

Hong, L., Summerfelt, A., Buchanan, R., O'Donnell, P., Thaker, G., Weiler, M., et al. (2009). Gamma and delta neural oscillations and association with clinical symptoms under subanesthetic ketamine. *Neuropsychopharmacology*, *35*(3), 632–640.

Humphries, M., Stewart, R., & Gurney, K. (2006). A physiologically plausible model of action selection and oscillatory activity in the basal ganglia. *Journal of Neuroscience*, *26*(50), 12921–12942.

Kaas, J. H., Merzenich, M. M., & Killackey, H. P. (1983). The reorganization of somatosensory cortex following peripheral nerve damage in adult and developing mammals. *Annual Review of Neuroscience*, *6*(1), 325–356.

Kaiser, M., Goerner, M., & Hilgetag, C. (2007). Criticality of spreading dynamics in hierarchical cluster networks without inhibition. *New Journal of Physics*, *9*(5), 110.

Kang, M., Spigelman, I., Sapp, D., & Olsen, R. (1996). Persistent reduction of GABAA receptor-mediated inhibition in rat hippocampus after chronic intermittent ethanol treatment. *Brain Research*, *709*(2), 221–228.

Larter, R., Speelman, B., & Worth, R. (1999). A coupled ordinary differential equation lattice model for the simulation of epileptic seizures. *Chaos: An Interdisciplinary Journal of Nonlinear Science*, *9*(3), 795–804.

Lazarewicz, M., Ehrlichman, R., Maxwell, C., Gandal, M., Finkel, L., & Siegel, S. (2010). Ketamine modulates theta and gamma oscillations. *Journal of Cognitive Neuroscience*, *22*(7), 1452–1464.

Lopes Da Silva, F., Blanes, W., Kalitzin, S., Parra, J., Suffczynski, P., & Velis, D. (2003). Dynamical diseases of brain systems: Different routes to epileptic seizures. *IEEE Transactions on Biomedical Engineering*, *50*(5), 540–548.

Lytton, W., & Omurtag, A. (2007). Tonic-clonic transitions in computer simulation. *Journal of Clinical Neurophysiology*, *24*(2), 175–181.

Lytton, W., Williams, S., & Sober, S. (1999). Unmasking unmasked: Neural dynamics following stroke. *Progress in Brain Research*, *121*, 203–218.

Nambu, A., Tokuno, H., & Takada, M. (2002). Functional significance of the cortico–subthalamo–pallidal "hyperdirect" pathway. *Neuroscience Research*, *43*(2), 111–117.

Neumann-Haefelin, T., Hagemann, G., & Witte, O. W. (1995). Cellular correlates of neuronal hyperexcitability in the vicinity of photochemically induced cortical infarcts in rats in vitro. *Neuroscience Letters*, *193*(2), 101–104.

Neymotin, S., Lazarewicz, M., Sherif, M., Contreras, D., Finkel, L., & Lytton, W. (2011). Ketamine disrupts theta modulation of gamma in a computer model of hippocampus. *Journal of Neuroscience*, *31*, 11733–11743.

Nudo, R. (2007). Postinfarct cortical plasticity and behavioral recovery. *Stroke*, *38*(2), 840–845.

Parent, J. M., Timothy, W. Y., Leibowitz, R. T., Geschwind, D. H., Sloviter, R. S., & Lowenstein, D. H. (1997). Dentate granule cell neurogenesis is increased by seizures and contributes to aberrant network reorganization in the adult rat hippocampus. *Journal of Neuroscience*, *17*(10), 3727–3738.

Phillips, W. A., & Silverstein, S. M. (2003). Convergence of biological and psychological perspectives on cognitive coordination in schizophrenia. *Behavioral and Brain Sciences*, *26*(1), 65–82.

Richfield, E. K., Penney, J. B., & Young, A. B. (1989). Anatomical and affinity state comparisons between dopamine D_1 and D_2 receptors in the rat central nervous system. *Neuroscience*, *30*(3), 767–777.

Schiene, K., Bruehl, C., Zilles, K., Q¨u, M., Hagemann, G., Kraemer, M., et al. (1996). Neuronal hyperexcitability and reduction of $GABA_A$-receptor expression in the surround of cerebral photothrombosis. *Journal of Cerebral Blood Flow and Metabolism*, *16*(5), 906–914.

Schweighofer, N., Han, C., Wolf, S., Arbib, M., & Winstein, C. (2009). A functional threshold for long-term use of hand and arm function can be determined: Predictions from a computational model and supporting data from the extremity constraint-induced therapy evaluation (excite) trial. *Physical Therapy*, *89*(12), 1327–1336.

Shema, R., Sacktor, T. C., & Dudai, Y. (2007). Rapid erasure of long-term memory associations in the cortex by an inhibitor of PKM zeta. *Science Signaling*, *317*(5840), 951–953.

Sporns, O., Tononi, G., & Kotter, R. (2005). The human connectome: A structural description of the human brain. *PLoS Computational Biology*, *1*(4), e42.

Suffczynski, P., Kalitzin, S., & Lopes Da Silva, F. (2004). Dynamics of non-convulsive epileptic phenomena modeled by a bistable neuronal network. *Neuroscience*, *126*(2), 467–484.

Sutula, T., Cascino, G., Cavazos, J., Parada, I., & Ramirez, L. (1989). Mossy fiber synaptic reorganization in the epileptic human temporal lobe. *Annals of Neurology*, *26*(3), 321–330.

Uhlhaas, P., & Singer, W. (2010). Abnormal neural oscillations and synchrony in schizophrenia. *Nature Reviews. Neuroscience*, *11*(2), 100–113.

Wurtz, R., Yamasaki, D., Duffy, C., & Roy, J.-P. (1990). Functional specialization for visual motion processing in primate cerebral cortex. [Cold Spring Harbor Laboratory Press.] *Cold Spring Harbor Symposia on Quantitative Biology*, *55*, 717–727.

Xie, X., Lancaster, B., Peakman, T., & Garthwaite, J. (1995). Interaction of the antiepileptic drug lamotrigine with recombinant rat brain type IIA Na+ channels and with native Na+ channels in rat hippocampal neurones. *Pflügers Archiv*, *430*(3), 437–446.

Yoshimura, Y., Dantzker, J. L., & Callaway, E. M. (2005). Excitatory cortical neurons form fine-scale functional networks. *Nature*, *433*(7028), 868–873.